Master Thesis
TVVR 17/5018

Investigation of groundwater resources

A case study in north-west Tanzania using remote sensing analysis and groundwater simulation

Cecilia Lundqvist

Division of Water Resources Engineering
Department of Building and Environmental Technology
Lund University

Investigation of groundwater resources

A case study in north-west Tanzania using remote sensing analysis and groundwater simulation

By:
Cecilia Lundqvist

Master Thesis

Division of Water Resources Engineering
Department of Building & Environmental Technology
Lund University
Box 118
221 00 Lund, Sweden

Water Resources Engineering
TVVR-17/5018
ISSN 1101-9824

Lund 2017
www.tvrl.lth.se

Master Thesis
Division of Water Resources Engineering
Department of Building & Environmental Technology
Lund University

English title:	Investigation of groundwater resources
Author:	Cecilia Lundqvist
Supervisor:	Magnus Persson
Examiner:	Rolf Larsson
Language	English
Year:	2017
Keywords:	Groundwater resources; Remote Sensing; Hydrologic budget; MODFLOW; Chonyonyo; Tanzania

Abstract

Globally 884 million people depend on unsafe drinking water, of which 159 million depend on untreated surface water (WHO, 2017). In Tanzania 44% of the population lack access to safe drinking water (WaterAid, 2017). Women and children in the small city of Chonyonyo, in Karagwe district are walking several hours a day for contaminated drinking water. According to a study, carried out in Tanzania, a shorter walk by fifteen minutes would increase a girls attendance to school by twelve percent (Unicef, 2013). The non-governmental organizations *Engineers without borders* Sweden and *Mavuno* Tanzania started a project to facilitate a water-supply system from a pumping well to the city of Chonyonyo. If successful the project would change the every-day life of women and children in the city, who would no longer have to collect and carry water the demanding path to the waterhole. The quality of the drinking water would increase and possible outbreaks of illness could be avoided. This thesis makes an attempt to estimate the potential of a groundwater resource by Chonyonyo city, and investigate two suggested borehole locations presented by *Mavuno*. The drainage basin for the two locations are studied and a hydrological budget for the larger basin has been calculated. The annual infiltration is used as input recharge for a groundwater simulation model in MODFLOW. The bulk part of remaining input parameters are estimated from local drilling and geomagnetic survey reports. The result from the hydrologic budget shows that 50% of annual infiltration would be exploited to meet the fresh-water demand. The sustainability of such exploitation is questionable. The MODFLOW model shows that for maximum withdrawal the limiting factor is the aquifers transmissivity and therefor several pumping wells need to be constructed with appropriate distance from one another. To know the withdrawal capacity of the aquifer test-pumping is recommended.

Keywords: Groundwater resources; Remote sensing; Hydrologic budget; MODFLOW; Chonyonyo; Tanzania

List of Figures

List of Tables

Contents

1 Introduction

Goal 6 of UN's sustainable development goals is to ensure clean water and available sanitation for all (UN, 2015). Globally 884 million people suffer every day from unsafe drinking water, of which 159 million use surfacewater for drinking (WHO, 2017). A lack of freshwater makes irrigation hard and therefore often result in a lack of food (WaterAid, 2017, Unicef, 2013). In Tanzania, the largest country in east Africa, 23 out of 52 million people are dependent upon unsafe drinking water for survival (WaterAid, 2017). Even though the country's groundwater resources are estimated to be sufficient the majority of the population lack access. 90 % of water collection for household use in Africa is done by women and children. According to a study, carried out in Tanzania, a shorter walk by fifteen minutes would increase a girls attendance to school by twelve percent (Unicef, 2013).

North-west Tanzania recharge Lake Victoria with run-off from its mountainous region. The area holds great potential in groundwater resources but the majority of the population lack access. Women and children in the small city of Chonyonyo, in Karagwe district are walking several hours a day for contaminated drinking water found in a waterhole shared with animals in a neighboring valley. Chonyonyo has 4000 households and is situated on a mountain ridge with demanding water carrying. The organization *Engineers without borders* have had several co-operating projects in Chonyonyo with the local non-governmental organization *Mavuno* regarding water supplement and education; Tanks for rainwater harvest have been installed in spring 2014 and a secondary girl-school opened in January 2016. The school is supplied with freshwater from a pumping well and during construction some of Chonyonyo's inhabitants collected water for household use from there. However since the school opened the water has been needed for the school facilities. To supply the city with freshwater and eliminate the water collection for women and children a solution is sought for. Now starts an investigation of the possibility to install a fresh water piping system from a pumping well in the valley (Engineers without borders, 2016). Two suggested locations for boreholes have been presented by *Mavuno*. Both locations are close to the waterhole where the inhabitants collect their water today. To estimate the resources of the aquifer, the groundwater quality and the design of the distribution system three master theses have been written for investigation. This thesis aims to give a recommendation for the location of the borehole as well as estimate if the aquifer can meet the freshwater demand from Chonyonyo.

2 Objectives and limitations

The two objectives of this survey is to estimate the aquifer by Chonyonyo city as a potential supply of freshwater for the Chonyonyos inhabitants assess which of two locations of boreholes, which have been suggested by *Mavuno*, to be preferable. The investigation is done in cooperation with the organization *Engineers without borders*, Malmo, Sweden, which has supplied most local information used in this report, such as magnetic survey and drilling reports and conditions for the population. A simulation model was made in MODFLOW to estimate impacts of a pumping well in the catchment. The MODFLOW version used is a student version from 1995, updated in 1999. Due to simulation restrains and limited known input data several estimations and modifications have been made for converging simulation. A field study was not carried out, which has proven to be a great loss for calibration data and valuable estimations. Ability to collect field data would make a calibration of image classification maps possible and therefore an assessment of reliability. The groundwater simulation would have been more reliable if surface water locations and water springs and flows in the valley were known. To visit the site would also increase a general knowledge of local conditions and culture behaviours.

3 Literature review

3.1 Remote sensing

Remote sensing is data about the earth surface obtained from a distance, by satellite or airplane. The information can be used to monitor natural resources and detect changes on the earth surface. The information obtained is electromagnetic energy, usually infrared from the earth's thermal energy or sunlight reflected on the earth surface (Richard and Jia, 2006).

3.1.1 The electromagnetic spectrum

Electromagnetic energy is wavelengths of different characteristics. Reflected sunlight gives indications of moisture, mineral, pigment and porosity of soils and other surfaces. The thermal energy holds information about the heat generated and emitted and can indicated the matureness of vegetation. Figure 1 presents the electromagnetic spectrum and the fraction which is visible for the human eye (400-00 nm) (Richard and Jia, 2006).

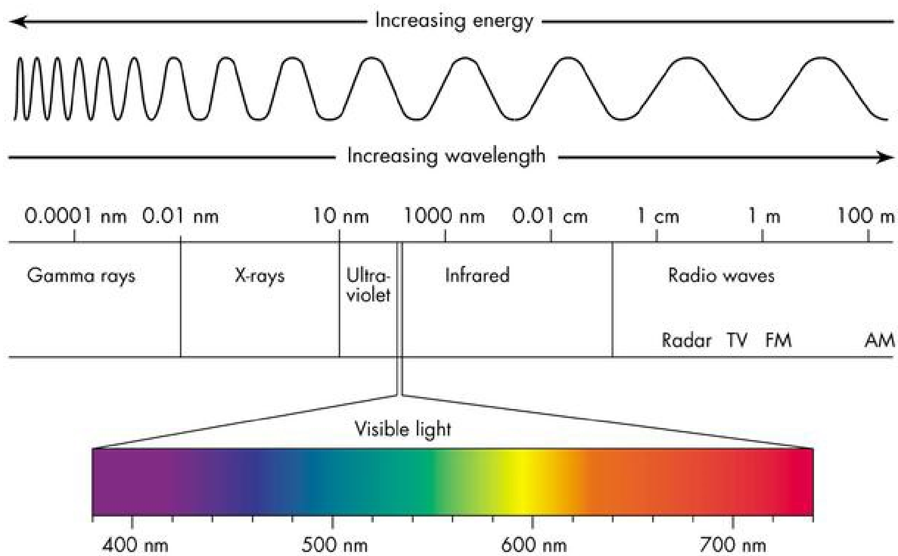

Figure 1: The electromagnetic spectrum with wavelengths visible to the human eye from 400 - 700 nm. Source: NASA, 2013

3.1.2 Image classification

In color images specific ranges in the electromagnetic spectrum is categorized as bands, were a range of electromagnetic waves are stored in one matrix. These bands are merged in multiband raster images. For analysis multiband raster images can be processed in GIS-software. For earth observations landcover type can be known by image classification. Software identify similarities in wavelength characteristics for every pixel in the image and an algorithm classify each pixel (Volker 1998). Classification of images are supervised or unsupervised. For supervised classification known areas are selected and a specific signature file is created for classifying the remaining image. Multiple merging and splitting of classes are made for a reliable result. For unsupervised classification the software identifies clusters where values of the spectral dimension is similar and classify the image from cluster similarities. Identification of surface cluster have to be made after an unsupervised classification. There are several different algorithms for image classification. For accuracy assessment samples in field are compared with the classified land cover. Accuracy assessment in image classification is most important (ESRI, 2017).

3.2 Hydrologic Budget

A hydrologic budget is accounting of the inflow to, outflow from, and storage in, a hydrologic unit, such as a drainage basin, aquifer, soil zone, lake, reservoir, or irrigation project. Additional water, such as precipitation, is added to the equation whereas leaving water, such as runoff, is subtracted (Fetter, 2001). Also added and subtracted water due to human activities needs to be considered, such as pumping and irrigation. Most components of a water budget can be measured or calculated. Below follows an account of the elements of a typical water budget.

The water budget equation by the surface looks as follows:

$$P - AE - R - S - I = 0 \tag{1}$$

Where P is precipitation, AE is actual evapotranspiration, R is runoff, S is storage due to uneven surfaces and I is infiltration. Mean annual waterbudgets usually have the unit mm/year.

3.2.1 Precipitation and measurements

Humid air is cold down to dewpoint and merge together on nuclears high up in the atmosphere. Once they merge to a critical size and weight they fall down through the atmosphere, and if they do not evaporate on the way, fall as precipitation on the earth surface (Fetter, 2001). In mountainous regions precipitation rates are usually higher than on flatlands since warm, humid winds are pushed upwards by the mountainside. The warmer air then cools down and as the saturation humidity value drops humid air condensate and fall as precipitation (SMHI, 2013). Precipitation is measured by meteorological stations with automatic or manual reading gauges. For a better spacial distribution data remote sensing can be used (Fetter, 2001).

3.2.2 Evapotranspiration

Evapotranspiration consists of evaporation from surfaces and transpiration from plants and is along with interception the total loss of water to the air in a watershed. Plants need water for photosynthesis and extract it from soil moisture and ground storage and in the process realise it to the air though the leaves. Precipitation that never reches the ground due to vegetation is known as interception (SMHI, 2017). The water loss due to transpiration depends on the density of the vegetation and is the bulk part of the evapotranspiration in most basins. Measurements of transpiration are complicated but evapotranspiration can be measured with a lysimeter. Potential evapotranspiration is the maximum theoretical amount of water loss due to evapotranspiration and can be calculated with known temperature. Thornthwaite introduced potential evapotranspiration as "the water loss, which will occur if at no time there is a deficiency of water in the soil for the use of vegetation" and found an expression for the potential evapotranspiration (see equation below). Even though the equation does not take into account the vegetation density it gives reasonable approximation. (Fetter, 2001; Zemadin et al. 2011)

$$Ti' = (\frac{Ti}{5})^{1.514}$$

$$PE_i = C * a * (\frac{10 * Ti}{I})^b \tag{2}$$

$$I = \sum_{1}^{12} Ti'$$

$$b = 6.75 * 10^{-7} * I^3 - 7.71 * 10^{-5} * I^2 + 1.792 * 10^{-2} * I + 0.4924$$

Where PE_i is potential evapotranspiration (mm/month) C is a constant depending on the region, a is a correlation factor for the day length and Ti is the mean temperature (degrees Celsius) of month i. Zemadim. B et al (2011) found in an empirical study carried out in Tanzania that the constant C mainly varies with altitude and mean temperature.

When plants suffer a shortage of soil moisture potential evapotranspiration is a theoretical term. The actual evapotranspiration is then limited by precipitation. To know the actual evapotranspiration Turc (1954) derived an expression for African basins that were later modified by Pike (1964). The equation is show below in Turc and Pike's method.

$$\frac{AE}{PE} = \frac{\frac{P}{PE}}{\sqrt{1 + (\frac{P}{PE})^2}} \tag{3}$$

Where AE is actual evapotranspiration (mm/month or year), PE is potential evapotranspiration (mm/ month or year) and P is precipitation (mm/month or year).

3.2.3 Runoff and infiltration

Percipitation that do not evaporate, infiltrate or lingers in depressions flows on the surface as runoff. Horton's equation describes the decrease of infiltration capacity during a rainfall event.

3.2.4 Horton's equation

Horton's equation states that the infiltration capacity of an earth material decreases over time. Infiltration capacity decreases with time until the infiltration capacity reaches an equilibrium. The function of time (t) and infiltration capacity (f_p) depends on the initial infiltration capacity (f_0), the final capacity (f_c) and a constant (k) representing the rate of decrease in infiltration capacity. The constant, which is scenario specific, depends on the surface structure, groundcover and hydrogeological properties of the soil. Equation 3 express Horton's infiltration equation (Fetter, 2001).

$$f_p = f_c + (f_0 - f_c)e^{-kt} \tag{4}$$

Both the initial infiltration capacity and the value of the constant k are in general difficult to determine (Fetter, 1994). Horton's equation assumes that the intensity of the rain is constant but infiltration also varies with rain intensity. Infiltration capacity during a storm has a lower than for a rainfall of less intensity, since the top layers of the soil gets saturated.

3.2.5 Rational method

The rational method is one of the most basic and used methods for estimating runoff. The equation assumes the whole basin to be contributing to runoff by the point of discharge. That is why the rainfall must have a duration longer than it takes for a raindrop to reach the discharge point from the most distant part of the watershed. The rational method is then the average rate of the rainfall times drainage-basin area and run-off coefficient. The runoff coefficient depends on surface structure and soil properties (Fetter, 2001).

The rational method:

$$Q = Aic \tag{5}$$

Where Q is peak runoff rate (m^3/s), A is drainage basin area (m^2), c is runoff coefficient and i is average rainfall intensity (m/s). The equation do not address decrease of infiltration capacity during a rainfall.

To know the run-off coefficient over a larger area a weighted run-off coefficient can be used. Equation 6 gives the weighted run-off coefficient:

$$C = \frac{\sum C_x A_x}{A_{total}} \tag{6}$$

Where C is the weighted run-off coefficient, C_x is the run-off coefficient for landcover x, A_x is the area of landcover x and A_{total} is the total area.

3.3 Groundwater

3.3.1 Earth materials

Slight movements of the earth's crust as well as physical and chemical weathering result in degradation of earth material. Voids are created in the rocks while grains are transported by wind and water to assemble in sediment deposits. The voids may be filled partly or fully by air, gas or water. The ratio between void and total volume is known as porosity. Even though a mineral has a high porosity it might not be transmitting water, the voids might not be interconnected or the size of the voids may be too small. When infiltration occurs interconnected voids of required size are temporarily filled with water and then drained by gravitation. The layer of the soil where saturation of voids is temporary is the unsaturated zone and the layers where the voids are filled with water is the saturated zone. An aquifer is a larger water-filled volume of connected voids with good transmissivity in the saturated zone, holding and transmitting water within the soil matrix. The water table is the plane between the unsaturated and saturated zone. The water head gives in m H_2O the pressure of the water body and water flows from a higher water head to a lower.

A soil with the same properties throughout the volume is called homogeneous, whereas a soil with spatial variations is called heterogeneous. In nature all soils are heterogeneous but for the commonly used groundwater equations homogeneous and isotropic conditions are assumed. An isotropic geological unit has the same properties in all directions (NAU, 2015).

3.3.2 Groundwater flow

Henry Darcy found out in the mid 1880s that the flow of water through a homogeneous, isotropic soil-bed depends on four parameters; the difference in height between the inflow and outflow, the cross-section and the length of the soil-bed as well as the properties of the soil. When all pores that could transmit water are filled a steady state condition is reached, the inflowing water then equals the outflowing water. Darcys law is found as the expression below.

$$Q = -KA\frac{(h_a - h_b)}{L} \tag{7}$$

Q= water flow (m^3/s)
A= cross-section (m^2)
$h_a - h_b$= difference in water head between inflow and outflow (m)
L= length (m)
K = hydraulic conductivity (m/s)

K is the hydraulic conductivity and represents the properties of the soil, the coefficient of permeability and is specific for each soil material. Most ground-water equations are derived from Darcy's law together with the first and second law of thermodynamics (Fetter 2001).

3.3.3 Aquifers and their characteristics

Due to differences in hydraulic conductivity earth materials are more or less permeable for groundwater flow. Materials with low hydraulic conductivity, such as clay and shales, acts as barriers for the groundwater as water flows slowly through. If water filled layer of higher hydraulic conductivity, as sand or cracks in stone, lays beneath a less permeable material the aquifer is confined. Such aquifers may be confined under pressure, means the potentiometric surface is higher than the top of the confined layer. A pressurized aquifer is called an artesian aquifer and when drilling a well water may flow without help. For excessive pumping in an artesian aquifer the water table drops and the pressure sinks (USGS, 2016).

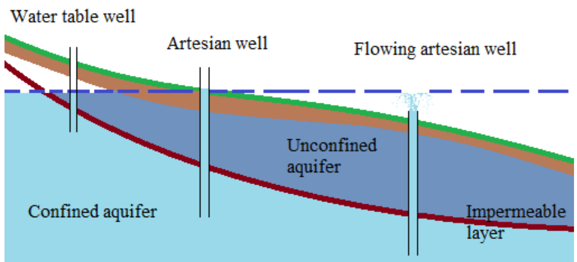

Figure 2: Aquifers and wells

If the ground material above the aquifer has a high permeability the aquifer is unconfined, meaning it can be recharge through infiltration through the unsaturated zone. Such aquifers are usually close to the land surface (Fetter, 2001).

3.3.4 Cone of depression

Water always flows from a higher waterhead to a lower. When pumping, the groundwater table gradually sink till the recharge area extent meets the demand for pumping. If there is no further draw-down of the water table with time the system has reached a state of equilibrium. The area affected by pumping is constant and called the cone of depression. As the hydraulic gradient is lowered by pumping water flows towards the well (Fetter, 2001). If the cone of depression is not constant the state is called transient. When test drilling pumping should be done until a steady-state condition is reached. The extent of the cone of depression depends on the discharge from pumping, aquifer thickness and hydraulic conductivity.

$$Q = (2rb\pi)K\frac{dh}{dr} \tag{8}$$

Q= water flow (m^3/s)
r= radial distance from the pumping well (m)
b= aquifer thickness (m)
K= hydraulic conductivity (m/day)
dh= h_0-h (initial hydraulic head - hydraulic head

3.4 Sustainable withdrawal

The traditional concept for sustainable groundwater withdrawal is pumping rate equal to the recharge rate through infiltration. If pumping exceeds infiltration the aquifer is depleted and therefore the withdrawal not sustainable. Groundwater is in constant motion and infiltrated water may be exfiltrating at a lower water head. Evaporation may decrease the groundwater table due to negative pressure or the aquifer may discharge through springs, streams and seeps downstream. Exfiltration and evapotranspiration from the aquifer is affecting the surrounding and downstream aquatic and ecological conditions. It may also affect downstream communities as human's and animal's water sources might be affected. Therefor Ponce, V (2007) argues that sustainable withdrawal of groundwater must be seen in a longer perspective where natural exfiltration from the aquifer is considered. A fraction of infiltrated water percolates to deeper layers. Since that fraction is not interconnected with surface waters nor exposed to evapotranspiration it might be considered as a sustainable withdrawal. For an annual global water balance, considering both surface and groundwater, 2% percolate to deeper groundwater storage (Ponce, V 2007). Since the figure is global, local values of deep percolations most be found to know the sustainable withdrawal for the specific aquifer.

Alley W.M et al (2013) argues that the population involved decides sustainability of groundwater extraction and acceptable consequences. They also declare that these consequences may take several years to surface, and if the groundwater system is directly interconnected with surface water bodies these might be depleted due to groundwater extraction. Therefore continuing collection and analysis of all depending parameters and well-designed simulation models can be used for groundwater management. For sustainability of groundwater resources Alley W.M et al (2013) list the following strategies: (1) where it is possible use alternative water-sources (2) have a spatial distribution of pumpage (3) increase recharge to the aquifer system by infiltration of surface waters or water reuse. They further states that only three factors can be considered when it comes to a sustainable management of a groundwater system; more water entering the aquifer, less water leaving or extraction of storge.

4 Background

4.1 Water resources in Tanzania

90% of water collection for household use in Africa is done by women and children, and contribute to an already unequal delegation of housework in African households. According to a study, carried out in Tanzania, a shorter walk by fifteen minutes would increase a girls attendance to school by twelve percent (UN, 2013). For 2016 the groundwater annual potential was 1952 m^3 per capita which is higher than the international acceptable volume of 1700 m^3. 23 out of 52 million people in Tanzania are dependent upon unsafe drinking water for survival (WaterAid, 2017). Even though the country's' groundwater resources are estimated to be sufficient the majority of the population lack access. A lack of freshwater makes irrigation hard and therefore often result in a lack of food (WaterAid, 2017, UN, 2013). The distribution of available groundwater is spatially over the country as well as each catchment. The Ministry of Water and Irrigation (2016) predicts that the water resources will decrease in the country due to population increase, climate change, water users conflicts, increasing social demand and lack of water managing. However latest hydrological reports have shown an increase in groundwater and surface water levels due to heavier rainfalls. Increase of pollution of watercourses due to unsafe sanitation practices in the catchments have also been recorded.

Tanzania, the largest country in east Africa, consist of nine larger basins (see Figure 3). Lake Victoria Basin recharge the second largest freshwater lake in the world. The southern and central part of the country receives unimodal precipitation from december-april whereas northern part of the country receives bimodal precipitation october-december and march-april. Annual precipitation varies between 1000- 2000 mm. Groundwater is found either in precambrian bedrock which underlay 75% of the country and has a maximum yield of 3 l/s, karoo sediments which include sandstones and conglomerates and has a yield varying between 0.1 and 5 l/s, coastal sedimentary which gives a yield between 1 and 6 l/s in limestone and 2.5 l/s as the highest yield in sandstone, volcanopyroclastics has an average yield of 11 l/s and alluvial deposits yielding between 0.2 and 2 l/s (Ministry of Water and Irrigation 2006). Groundwater quality is usually drinkable, except for the coastal aquifers which has salinity problems due to saltwater intrusion.

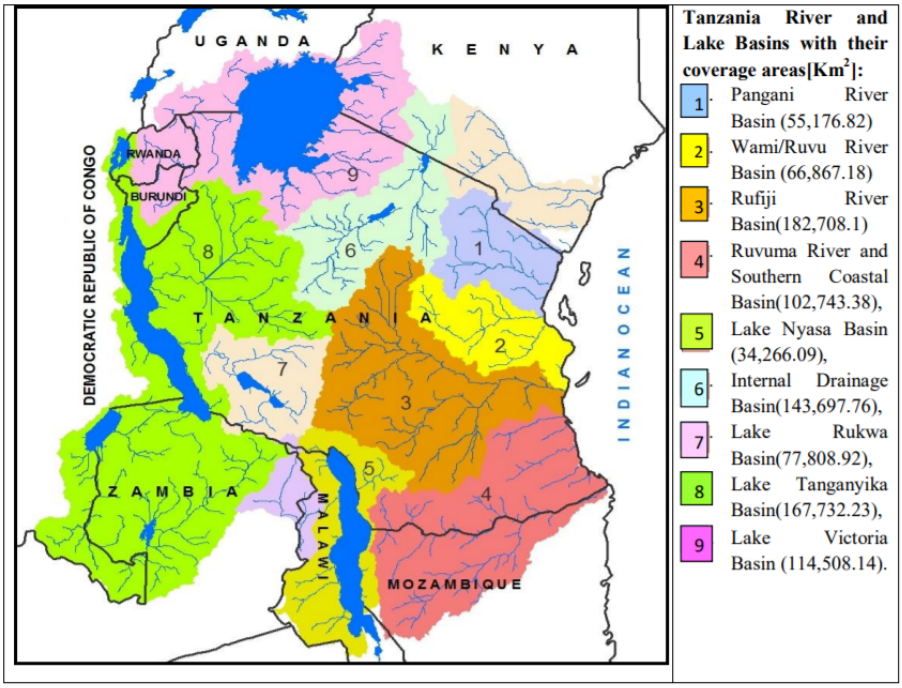

Figure 3: Tanzania's nine River Basins (Source: Ministry of Water and Irrigation, 2016)

4.2 Area of interest

The studied valley is a subcatchment in Lake Victoria Basin, one of the nine basins in the country (Ministry of water and irrigation, 2016). The area studied is a valley by the city Chonyonyo in the district of Karagwe, in north-west Tanzania. Karagwe district is situated between Rwanda in the west and Lake Victoria to the east and is a river complex and a part of the Kagera river basin. Kagera river basin reaches across Burundi (23%), Rwanda (34%), Tanzania (35%) and Uganda (8%) and is the most important contribution for recharging Lake Victoria (FAO, 2014).

Figure 4: The map shows the location of the village Chonyonyo in north-west Tanzania, in Lake Victoria River Basin and a close-up map of the study-site. Modified from USGS - Earth Explorer 2016

The area by Chonyonyo is characterised by mountainous ranges, and the valley studied has a bottom level at 1380 amsl and the highest point at 1630 amsl (USGS Earth explorer, 2016). The city of Chonyonyo consists of 4 000 households (Engineers without Borders, 2016) and the average household size in Tanzania was 4.8 in 2012 (UNPF, 2013) therefore the total population of Chonyonyo can be estimated to about 19 000 inhabitants.

4.3 Climate data, Karagwe district

The climate is sub-humid to semi-arid with two dry seasons, January-March and June-October and two wet seasons, September-December and April-May, with the bulk precipitation in November and April (Tanzania Meteorological Agency, 2015). The mid temperature is evenly around 20 degrees throughout the year. Monthly average maximum and minimum temperature and average monthly precipitation from Tanzania Meteorological Agency weather station 9 km north of the study site is presented in Figure 5 below. The data series are collected between 1968 and 2014. Total monthly precipitation and monthly average temperature is presented in Table 1.

Table 1: *Monthly average temperature from collected average min and max temperatures and precipitation from Tanzania Meteorological Agency (2015).*

	Jan	Feb	Mar	Apr	May	Jun	Jul	Aug	Sep	Oct	Nov	Dec
P [mm]	65	71	124	151	91	5	4	19	60	109	123	116
Tmid [C^o]	20	20	20	20	19	20	20	20	20	20	20	20

According to the climate data from Tanzania Meteorological Agency (2015) the driest period is during summer from May to August with almost no precipitation during June-July. During October to December the precipitation is twenty times the volume compared to the drier season.

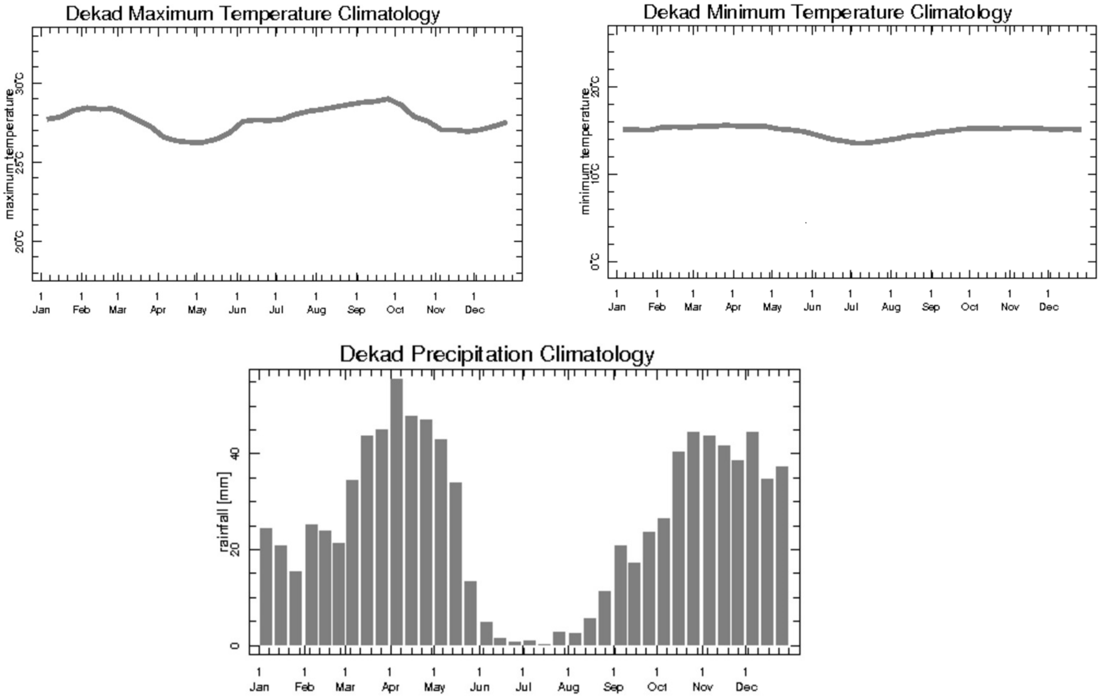

Figure 5: Monthly average temperatures (max and min) and precipitation from a climate station 9 km north of the study site with collected data between 1968-2014.

4.4 Hydrogeology in Chonyonyo and Karagwe district

Engineers without borders have in a cooperating project with the local non- governmental organization *Mavuno* finished building a school supplied with freshwater from a pumping well. Before the well was constructed *Engineers without borders* and *Mavuno* had a geomagnetic and resistivity survey done by a drilling company based in Dar Es Salaam (Shinhu,R. 2016). All test sites are situated on the mountain ridge by or in the city of Chonyonyo. Groundwater potential in the valley is expected to be greater, therefor the suggested boreholes for the new well is situated in the valley (see Figure 6). The survey consist of a general geological survey of the area and geomagnetic and resistivity survey for estimating groundwater potential. The geomagnetic intensity indicated groundwater levels at varying depth from 20 meters to 130 meters below the land surface. The coordinates for the survey sites, depth to potential groundwater and distance from suggested borehole locations are found in the table below. The first three sites are close to and in the city of Chonyonyo and site 4 is on the other side of the river basin.

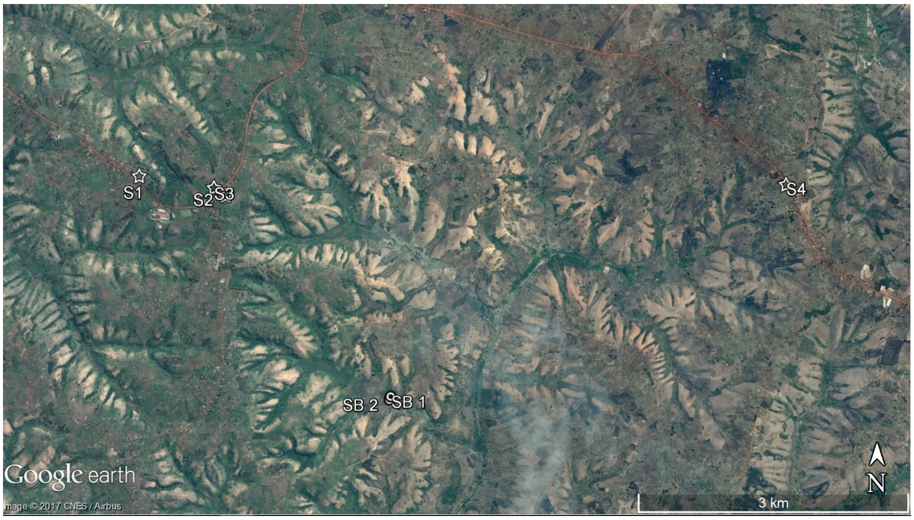

Figure 6: Location of investigated sites (S) made before Mavuno Girls Secondary School in Chonyonyo and suggested boreholes (SB) for construction of a new well (Source: Google Earth Images, 2017)

Table 2: *Survey-site coordinates, depth to potential groundwater level and distance from suggested borehole locations*

	Latitude	Longitude	GW [m]	Distance [km]
Site 1	-1.569664	31.055898	62	3,7
Site 2	-1.571598	31.064548	80	3
Site 3	-1.570855	31.063381	50	2,9
Site 4	-1.570492	31.120077	20	5

The basic geological survey from Shinhu,R. (2016) report stated that the valley is predominantly precambrian metasedimentary rock from superficial deposits of reddish brown silt soil and weathered shales. The report further states that Karagwe district is characterized by Karagwe Ankolean system which compose of sandstone, quartzites, shales and mudstones which is further confirmed by FAO (2017). According to Shinhu,R. (2016) possible extractions of groundwater are from weathered sandstones/quartzites and fractured shales. FAO (2017) describes the area as well drained surfaces with greener flood lines and annual infiltration estimates 270 mm (out of annual average precipitation of 900 mm) in Karagwe Ankolean region. The basin in question has elevation fall from 1380 masl to 1620 masl in less than 2 kilometers. Direct analysis of remote sensing data along with above stated information indicates erosion on mountain sides and deposits in slower flowing waters downstream.

The same water- and drilling company made another report with multi test-pumping 32 km north-east of Chonyonyo on a floodplain 1200 m asl (Ramadhani, M.M 2013). Six test pumpings were made at six different pumping locations with a varying yield of 142 m^3/day to 26 m^3/day. The depth to a transmitting layer varied between 69 meter to 93 meters were the deeper depths gave a greater yield. The survey include a detailed logging of geological layers and five out of six test-drillings shows a clay layer above fractured limestone, indicating a confined aquifer. Even though the test-pumpings are made 32 km away from the study-site on a floodplain the pump sites are close to typical Karagwe Ankolean topographical landscape.

4.5 Surface water and vegetation

An account regarding surface water and vegetation in the studied valley was given by a *Mavuno* worker:

"During autumn and winter the valley is full of springs and running water. Some years, during the wet-season, the flow from the valley is wide and deep whereas other years the flood bed is almost dried out. It is a green place with fern plants, ficus spp, bamboo, reeds, elephant grass and trees that naturally grows in the valley. The dominated farming crops are beans, maize, groundnuts, soyabeans, cassava, sweet potatoes and even banana plants, the yield differ from year to year depending on precipitation."

FAO (2017) states further that trees in the area are ficus, albizzia, A. polycantha, Acacia Kirki and that the permanent watercourses, like the main river Kagera with tributants are permanently greened by forest. The studied basin is a subcatchment to a river recharging Lake Mujunju 20 km south-west of the studied site. Lake systems and swamps are common in Kagera basin and provide habitat for globally threatened animals.

5 Methodology

For investigation of groundwater resources topographic and 3-band images from remote sensing data was used in ArcMap (ASTER GLOBAL DEM and Landsat 8 program). The remote sensing analysis gave catchment extent. A weighted run-off coefficient was calulcated using equation 6. With measured percipitation, calculated actual evapotranspiration and caluclated runoff infiltration was found with a hydrological budget. The monthly infiltration values were used as recharge for a groundwater simulation model. For basic knowledge of the area a brief online interview was made with a *Mavuno*-worker, some information may have been lost in translation but an interpretation of the responses are found in chapter *4.5 Surface water and vegetation*, for a full account contact the author.

5.1 Watershed extent

To investigate the recharge area an elevation map from ASTER GLOBAL DEM was analyzed in ArcMap, found at USGS, Earth Explorer (2016). A flow accumulation map was created to see the area contributing to runoff. Then the two locations suggested for boreholes were added and the area contributing to runoff calculated in ArcMap. The catchments were then analysed with landcover classification.

5.2 Landcover analyses

To determine the landcover in the watershed remote sensing from Landsat 8 was used (USGS, Earth explorer 2016). The land cover was defined with a supervised classification and the maximum likelihood algorithm. Accuracy assessment was made manually with corresponding likeliness to the original 3-band raster image until the correlation was satisfying. The areas of each landcover was used for further analysis.

5.3 Hydrologic budget

A weighted run-off coefficient, C_W was found through Equation 6 using the landcover areas and estimated run-off for each landcover type. Since neither intensity nor duration of the rainfalls were known run-off were calculated as follows:

$$R_i = P_i C_W \tag{9}$$

Where R_i is run-off (mm) for month i, P_i is average precipitation (mm) for month i (found in Table 1) and C_W weighted run-off coefficient for the catchment.

Thornthwaite equation was used to found evapotranspiration with constant C given by Zemadim. B et al (2011) empirical study in Tanzania and mean temperature from Table 1. Since Zemadim. B et al (2011) argued that C depends mostly on altitude and mean temperature, C was in this investigation set to the same value as for a similar altitude site Zemadim et al (2011) studied in there report (climate station Iringa). The value of C varied with mean temperature for each month (see *10.2 Appendix II*). Actual evapotranspiration was then found with Turc and Pike method. A hydrologic budget was set up for the catchment and known or calculated monthly data for precipitation, actual evapotranspiration and run-off gave an estimation of monthly and annual infiltration value in mm (see *10 Appendix II*). For this study the storage in the water budget equation, due to an uneven surface, was neglected. Infiltration value was used as recharge for a groundwater simulation model in MODFLOW.

5.4 Groundwater modelling

A groundwater simulation model was made to estimate the impacts of extraction and evaluate limiting factors. Two suggested locations for boreholes were provided by Mavuno projects, the locations are presented in Table 3 (see Figure 6 for suggested borehole (SB) locations).

Table 3: *Suggested borehole locations, WGS84 37S.*

	Latitude	Longitude
Suggested site 1	-1.591780	31.080720
Suggested site 2	-1.571598	31.064548

5.4.1 Conceptual model

The study site was conceptualized for simulation. The estimations and simplifications are shown in the Figure 7. The aquifer was set to be a confined aquifer with varying depth across the model. The aquifer was assumed to be confined since the geologic logging from the drilling tests (Ramadhani, M.M 2013) showed a confining layer of clay. Hydraulic conductivity of layer 1, which was assumed to be shales was set to 10^{-8} m/day and for layer 2, which was assumed to be fractured shales 10^{-6} m/day (Heath, 1983). The bedrock below layer 2 was by default set to a no-flow boundary, since water flows though the bedrock with difficulty. The catchment boundary was also set to a no flow boundary. The catchment boundary is a water-divider and the groundwater was estimated to flow in the same direction as the surface water. Depth to layer 2 was set to 80 m on hilltops and 40 m in the lower part of the valley, with a varying thickness of 10 m to 30 m. Values are based on the reports from Shinhu, R. (2016) and Ramadhani, M. M., (2013).

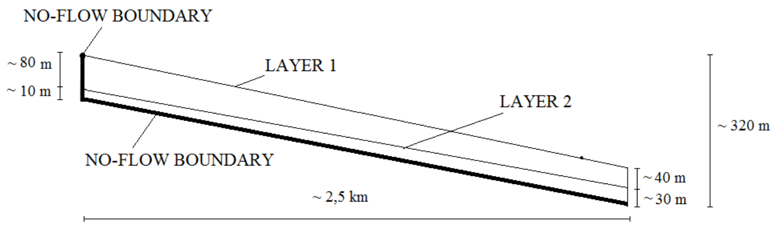

Figure 7: Conceptual model. Elevations and layer thickness is varying with cross-section.

5.4.2 Simulated model

Simulations were made in MODFLOW. MODFLOW is a groundwater program first launched in 1995. The student-version used in this thesis was updated in 1999. The conceptual model was simulated with some modifications due to simulation model restrains. The model was set up with a grid of 40·40 cells each cell represent approximately 40 m ·40 m. Two layers were added to the simulation. The layer consisting of the altitude values was retrieved from the topographical map from the satellite program ASTER GLOBAL DEM (USGS- Earth Explorer, 2017). From the topographic matrix a second layer was extrapolated and manipulated according to equation in *9 Appendix I*. A basemap was imported from ArcGIS (modification of Figure 12) to know the landcover and catchment extent. Cells not included in the catchment area was set as inactive. Pumping wells were added in the suggested locations to see differences due to location. To know aquifers limitation pumping rates were increased until cells closest to the well dried out. Pumping rates started at 60 m^3/day and increased. The screening depth was set to the same depth as layer 2 (30 m), see Figure 8.

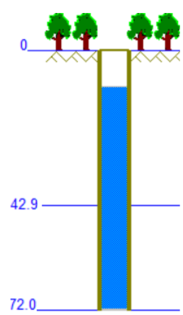

Figure 8: Screen-depth and piezometric head at drilling location 1.

5.4.2.1 Recharge

For a converging model monthly infiltration values could not be used, since values during summer drained the model and calculations did not converge. The simulation was made with total infiltration of 69 mm for 8 months in a row, followed by a dry season of total infiltration of 20 mm for 4 months which adds up to the annual infiltration (89 mm/year). To simulate the differences in infiltration due to landcover and slope two infiltration zones were used, one with hillslopes and a flatter landcover area see Figure 9 for sectioning. The run-off coefficient (c) was set to 0,8 and 0,64 for hillslopes and flatter lands respectively. The infiltration ratio was found by the ratio of weighted runoff coefficient for the land-cover types in the two different recharge areas.

5.4.2.2 No-flow and constant head boundary

By default inactive cells are set to no-flow boundaries in MODFLOW (USGS 2005, p. 79/253) as is model border. A constant-head boundary of 1332 masl was introduced to drain the model by the natural discharge in layer 2, see Figure 9. Unrealistic values of water table were found by uneven model edges therefore constant head boundaries were introduced were groundwater levels were known on the mountain ridge (1530 masl) as well as an estimated groundwater level by the north-east side of the catchment (1450 masl). Constant head is marked in red in the Figure 9 (middle and left). A river with a river stage depth of 0,2 m and conductance of 3 m^2/day was introduced for simulation of natural drainage. The two locations for borehole was added and different extraction rates were tried. The simulated model for each of the two layers is shown in the figure below. Hydraulic conductivity have the same properties at all locations $K_x = K_y = K_z$.

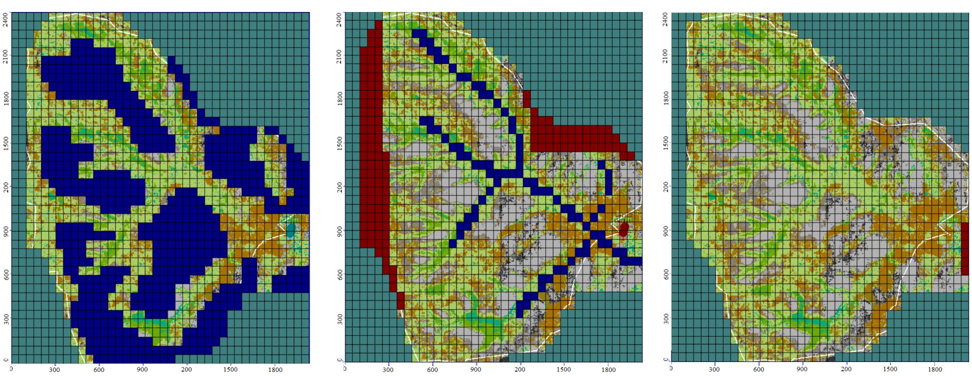

Figure 9: Simulated model. From left: different recharge areas in blue and transparent, hydraulic boundary (red) and river boundary (blue) for Layer 1 and hydraulic boundary (red) for Layer 2

6 Results

6.1 Catchment area

In Figure 10 accumulated runoff is presented. Each pixel value correspond to the amount of cells connected upstream the catchment, with a resolution of 30·30 meters. The colors in the legend show the contributing run-off area in square kilometers.

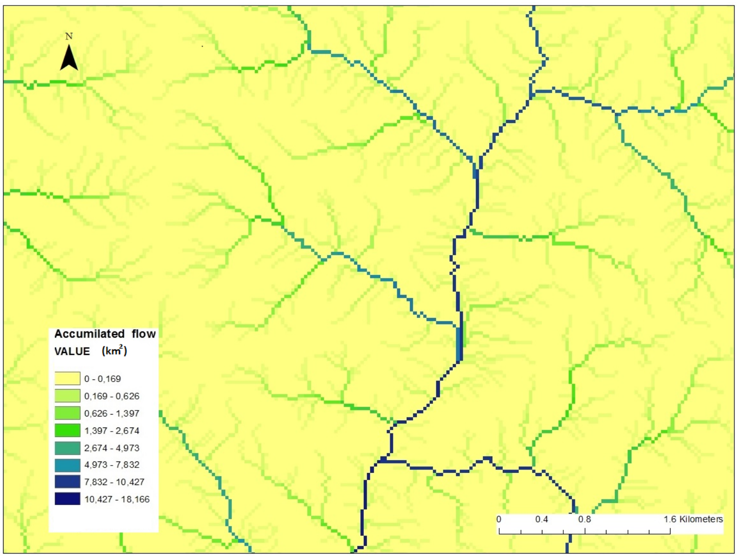

Figure 10: Shows the flow accumulation map of the river catchment. The colors in the legend represent the different contributing run-off areas in square kilometers.

6.1.1 Investigation of suggested borehole locations

The calculated watersheds for the two boreholes are presented in Figure 11. The contributing basin area for location 1 and location 2 are shown in white and black, respectively. The contributing runoff area for a well at suggested location 1 is 3,09 km^2 whereas the basin of a well located at the second suggestion is 0,02 km^2.

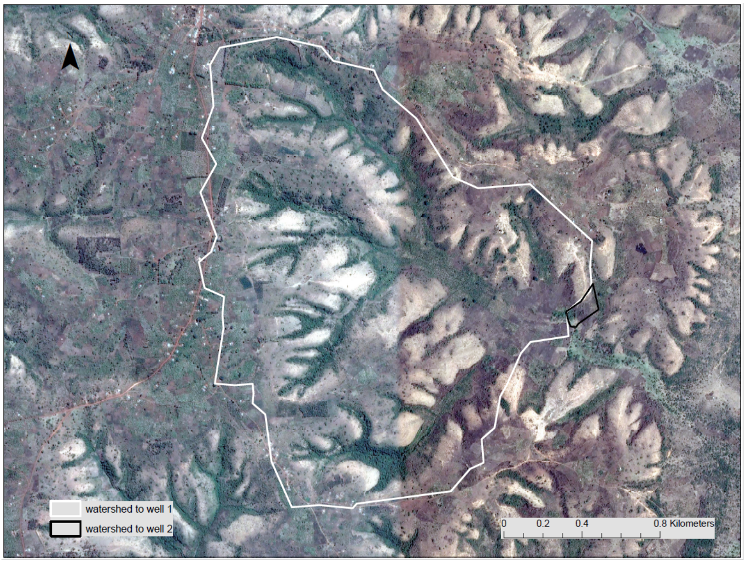

Figure 11: The figure shows the extent in the geographic terrain of the two river basins contributing to the two suggested locations for boreholes, the larger in white and the smaller in black.

6.2 Landcover analysis

The results from the supervised classification is shown in Figure 12. Each color represent a land cover type, the land cover types are presented with respect contributing areas in Table 4. The white and black lines shows the catchment borders for the two suggested locations. Only the larger catchments contributing areas in presented in Table 4 below.

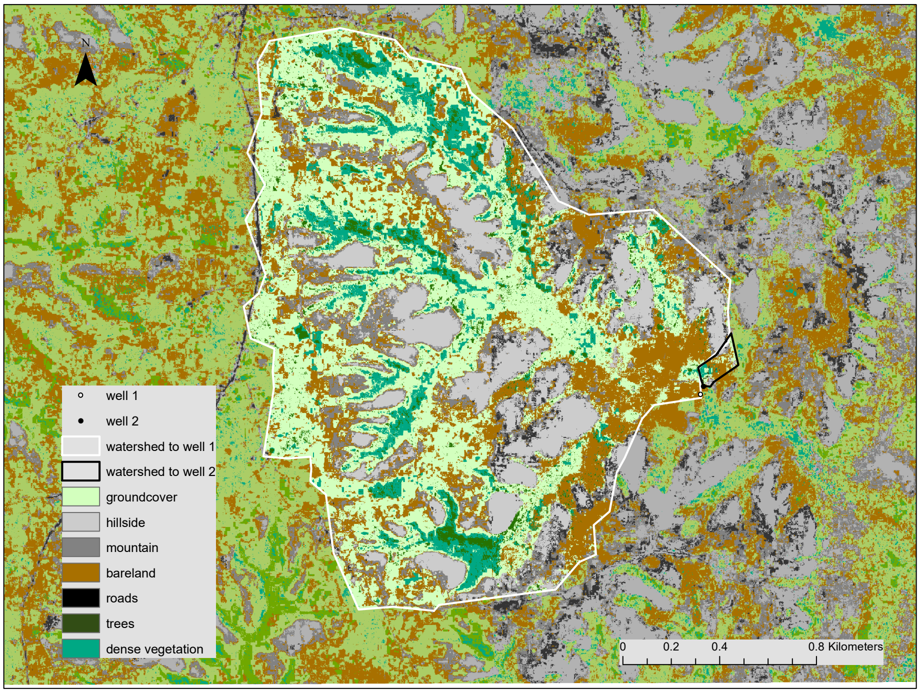

Figure 12: The river basins for the two suggested borehole locations. The white line indicates the basin border of suggested location 1 and the black of suggested location 2. The colors represent seven different land cover classes within the basins

Table 4: *Surface area, runoff coefficient and reduced area for each landcover class for the larger basin analysed.*

	Surface area (km^2)	Run-off coefficient	Reduced area (km^2)
Hillside	0,52	0,8	0,41
Mountain	0,31	0,8	0,25
Bareland	0,63	0,35	0,22
Roads	0,07	0,7	0,05
Low vegetation	1,17	0,1	0,12
Dense vegetation	0,27	0,1	0,03
Trees	0,12	0,1	0,01
Total area	3,09		1,09

The values of the runoff coefficient was taken from Fetter (2005) and Svenskt vatten (2016). The weighted runoff coefficient is 0,35 which gives a reduced area of 1,09 km^2 Hillside estimates consist of steep shales, mountain of shales, bareland of silt soil, roads of lateritic soil (Shinhu, R., 2016).

6.3 Infiltration analysis

Only the larger catchment iniftration area was caluculated. Infiltration analyses were done using a hydrological budget. Infiltration per month is presented in Table 4 below with a total annual infiltration of 89 mm.

Table 5: *monthly precipitation (P), evapotranspiration (AE), difference (P-AE), runoff (R) and infiltration (I) in Karagwe*

	P	AE	Δ	R	I
Jan	65	61	4	1	2
Feb	71	66	5	2	3
Mar	124	102	22	8	14
Apr	151	114	37	13	24
May	91	80	11	4	7
Jun	5	5	0	0	0
Jul	4	4	0	0	0
Aug	19	19	0	0	0
Sep	60	57	3	1	2
Okt	109	93	16	6	10
Nov	123	101	22	8	14
Dec	116	97	19	7	12
Annual total I [mm]					89

6.3.1 Sustainable withdrawal

A reduced catchment area of 1,09 km^2 gives a infiltration volume of 275 702 m^3/year. The water demand is 146 000 m^3/year for 4000 households and average 4,8 pers/household (WHO, 2017) meaning 53 % of the aquifers potential would be exploited. According to Ponce., V (2007) a sustainable outtake should be around 2%, which would only supply 1 % of Chonyonyo's population.

6.4 Groundwater modelling

Below is a presentation of the groundwater simulation results. All simulations were made with steady-state condition with varying recharge rates, MODFLOW takes the output values of the first recharge period as input to the next recharge period until steady-state is reached for each period. Figure 13-14 shows natural condition, without pumping simulations, Figure 13 shows plane view with water head isolines and Figure 14 shows cross-section for a specific location to see the water head level ini west-east direction. Each scenario presented during this section shows first effects when pumping at suggested borehole location 1 and then at suggested borehole location 2 (see Table 3 and Figure 6 for coordinates and definitions). Figure 15-20 shows results from pumping at 120 m^3/day (Figure 15-17) and 130 m^3/day (Figure 18-20). Apparent changes to the water table is shown first at pumping rate 120 m^3/day. At 130 m^3/day the cells closest to the active pumping well dries out due the cone of depression. To visualize the decrease of the water head due to pumping each scenario shows both plane view and a cross-section. The cross-section is taken at the same location for all scenarios, Figure 13 shows cross-section location. The cross-section further shows water head level across the model (west to east), where the area above the water head is shown in blue and the area below the water head is shown in white.

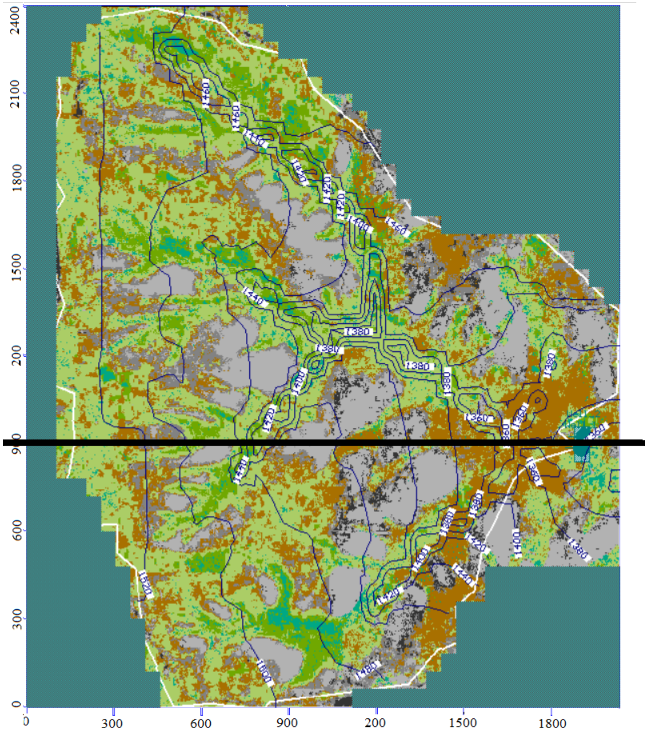

Figure 13: *Waterhead isolines, natural condition. Black line shows which cross-section Figure 14, 16-17, 19-20 shows.*

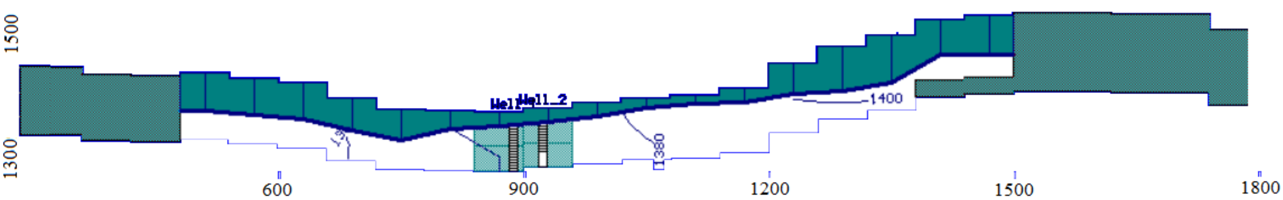

Figure 14: *Profile from north to south, natural condition. The area above the water head is colored in blue and below the water head is colored in white. Figure 13 shows where the cross-section is taken.*

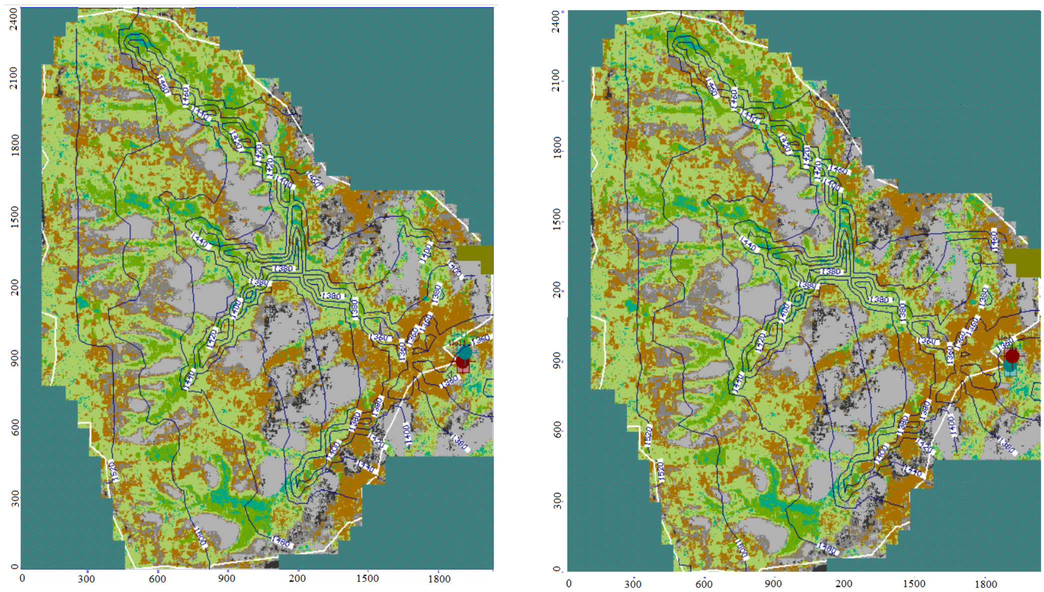

Figure 15: Comparison between pumping well at location 1 or well at location 2 with an extraction rate of 120 m^3 per day.

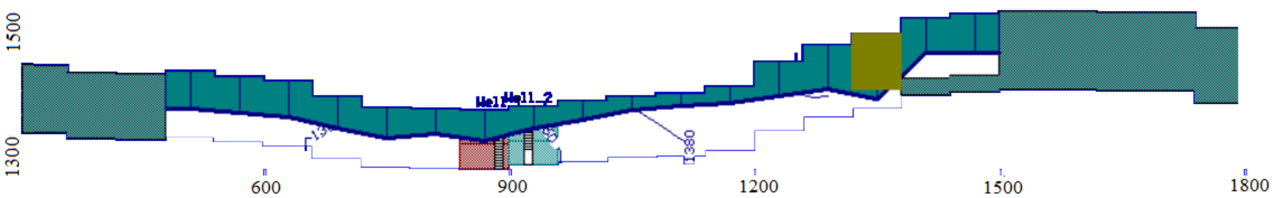

Figure 16: Profile from north to south, pumping with well 1 at a rate of 120 m^3 per day. The area above the water head is colored in blue and below the water head is colored in white. Figure 13 shows where the cross-section is taken

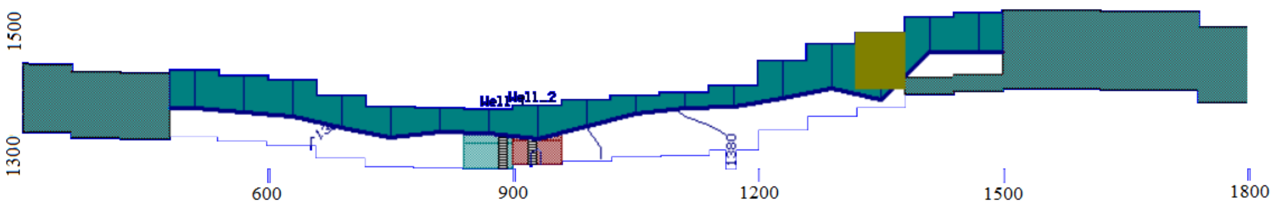

Figure 17: Profile from north to south, pumping with well 2 at a rate of 120 m^3 per day. The area above the water head is colored in blue and below the water head is colored in white. Figure 13 shows where the cross-section is taken

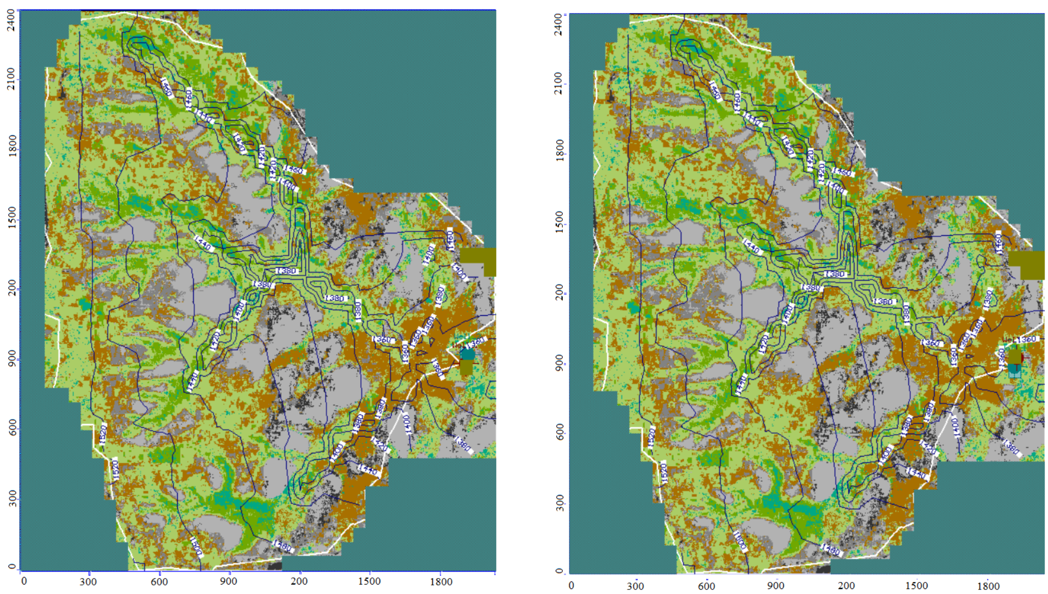

Figure 18: Comparison between pumping with well at location 1 or well at location 2 with an extraction rate of 130 m^3 per day.

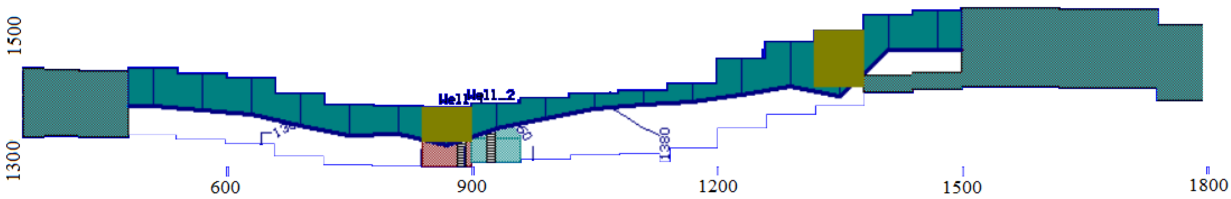

Figure 19: Profile from north to south, pumping with well 1 at a rate of 130 m^3 per day. The area above the water head is colored in blue and below the water head is colored in white. Figure 13 shows where the cross-section is taken

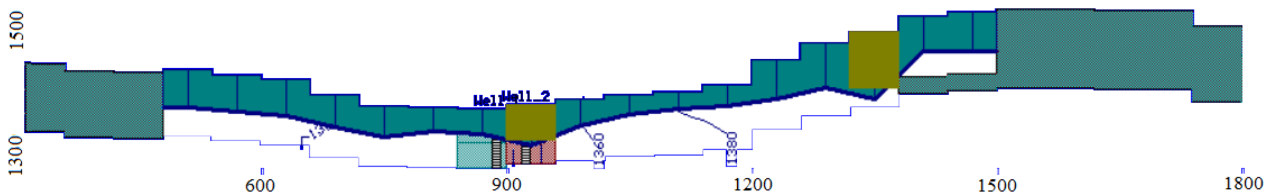

Figure 20: Profile from north to south, pumping with well 2 at a rate of 130 m^3 per day. The area above the water head is colored in blue and below the water head is colored in white. Figure 13 shows where the cross-section is taken

6.4.1 Water budget and flow direction

A flowchart shows volume/time in recharge (IN) and discharge (OUT). A typical flowchart generated during simulation is presented in Figure 21. Summarized constant head boundaries contribute with 54 m^3/day (OUT-IN) drainage of the model. The flowchart shows inflow and outflow during one day. The chart stacks without values are non-existing.

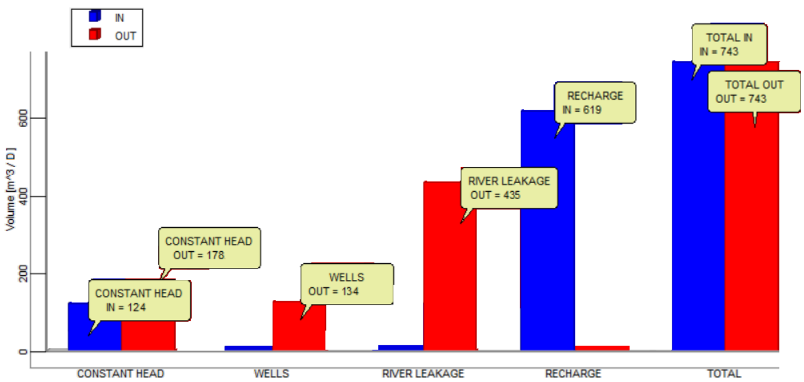

Figure 21: Flowchart, well 2, extraction 130 m^3/day

Figure 22 shows flow velocity (to the left) and magnitude (to the right) for layer 2 pumping at 130 m^3/day. The groundwater flows towards the constant head, acting as draining cells at layer 2, indicating that the constant heads applied to regulate unrealistic values in layer 1 does not affect the direction of the groundwater flow. The equipotential lines further confirms the groundwater flow towards the well and draining boundary in layer 2. Figure 23 shows flow velocity (to the left) and magnitude (to the right) in a natural environment, without pumping. No significant differences can be seen in a pumping or non pumping environment.

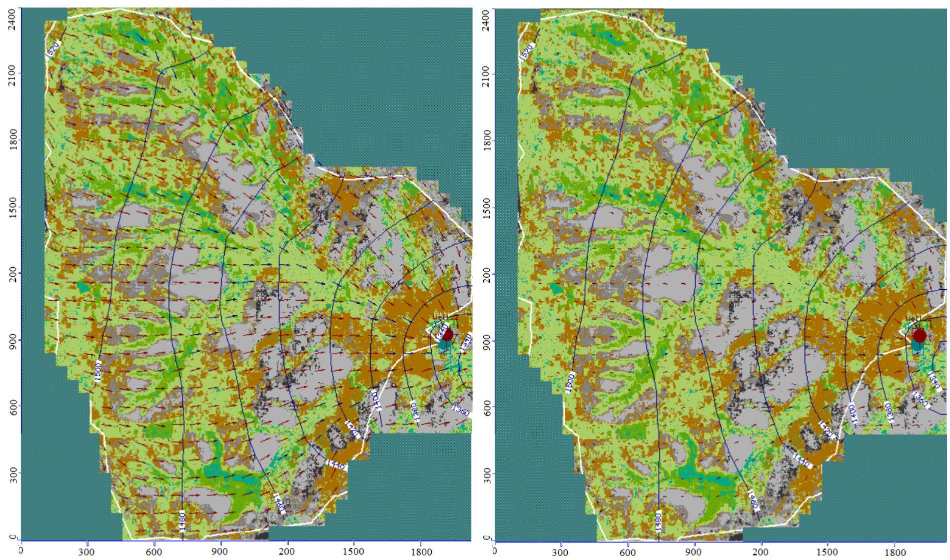

Figure 22: *Velocity direction and magnitude (arrows) and equipotential lines (isolines), well 2, extraction 130 kbm/d*

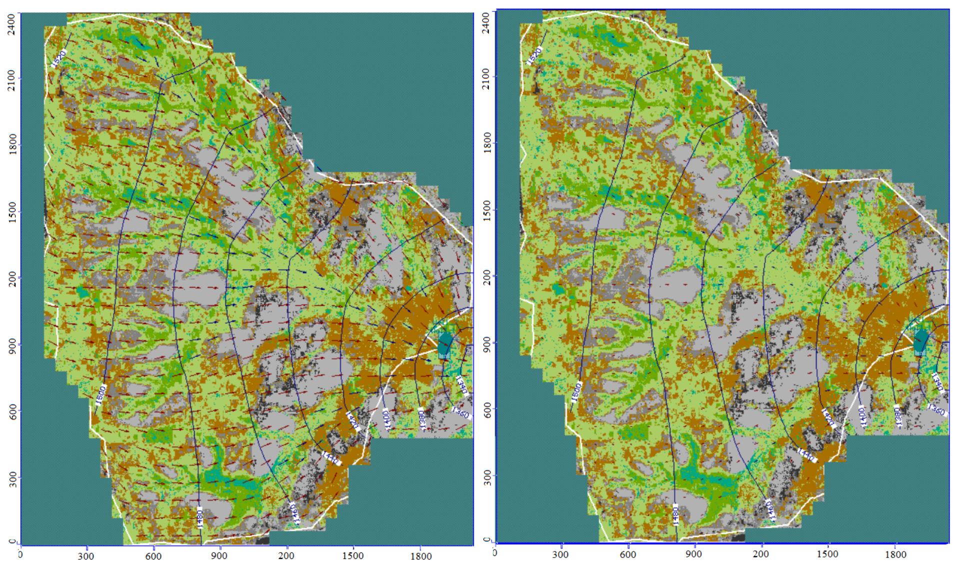

Figure 23: *Velocity direction and magnitude (arrows) and equipotential lines (isolines), natural condition*

7 Discussion

Since no field-work was carried out many parameters had to be estimated for infiltration analysis the setup of the groundwater simulation model.

7.1 Infiltration analysis

According to investigation annual infiltration volume is enough to supply Chonyonyo's population with freshwater. To meet the demand from the estimated population of Chonyony 50% of the aquifers annual infiltration would be exploited. The meteorological data provided by Tanzania Meteorological Agency (2017) are monthly and not specific for each rainfall event. Therefore differences in infiltration capacity for rainfall intensity or during (see chapter *2.3.4 Horton's equation*) is not taken into consideration. Signs of erosion indicates high rainfall intensity, why infiltration might be overrated. According to FAO (2013) annual infiltration to the saturated zone is 270 mm out of 900 mm precipitation in Karagwe district. Considering the infiltration capacity on the floodplains and slowly meandering rivers downstream the steep hills would have a lower infiltration capacity. The account from the local *Mavuno* worker indicate large ratio of run-off when explaining the wide and deep river in the valley which further speaks for a high run-off and therefore lower infiltration rate. Regarding landcover classes accuracy assessment no sampling for accuracy was possible but satellite images were accurately investigated manually for calibration, however due to similarities landcover units were easily confused.

7.2 Location of borehole

The remote sensing analysis showed that the catchment for the two suggested borehole locations varied dramatically. One suggested site (-1.591780, 31.080720) is a subcatchment to the other (-1.592100, 31.080610), the latter being 190 times the size of the first. That is probably due to local topographical formations that creates a sheltered area for the subcatchment. The borehole location did not matter in MODFLOW simulations, perhaps because the resolution of the MODFLOW model is less refined that for the maps analysed in ArcMAP. The two catchments could also be extracting from the same aquifer, since the depth to water transmitting layer (in simulation) is deep (20 m). The borehole with a contributing catchment of 3 km^2 is recommended since variables are uncertain, if that locations is regularly flooded during monsoon contaminated water could infiltrate the well. In such case the smaller catchment may be preferable, then test-pumping is recommended before construction.

7.3 Groundwater model

Due to multiplied unknown parameters the groundwater simulation model should only be seen as an indication. There was a fine line between a flooded and a drained model as simulations were sensitive to changes. Adjustments to the model had to be made for every change in a parameter for the model to convey. Once realistic results were found the simulations showed transmissivity of the aquifer to be the limiting factor for extraction. Pumping continued til a maximum extraction of 60 m^3/day to 140 m^3/day, yield depending on aquifer thickness. At first cells by applied constant hydraulic head in layer 2 dried out (Figure 15-17) and then cells by the pumping well dried out (see Figure 18-20) . Since the applied constant heads at layer 2 were set to regulate unrealistic waterhead values in a natural condition the drying out of cells by the constant heads were ignored. Aquifer thickness investigated were known aquifer depths from the magnetic survey by Chonyonyo (Shinhu, R. 2016) and the drilling report 30 km north-east of the study site (Ramadhani, M. M. 2013). However none of the made reports were done in a similar site as the two suggested borehole locations.

7.3.1 Pumping

If the project is implemented the limiting factor for groundwater extraction will, according to simulations, be the transmissivity of the aquifer materials (fractured shales). Therefore several pumping wells needs to be constructed in the valley. To supply the city with freshwater 400 m^3/day need to be extracted. With a rate of 130 m^3/day that would require three pumping wells in the valley. These should be placed so that the cones of depression are not interfering significantly with one another, according to simulation approximately 40 m. Even though a pumping rate of 130 m^3 is highly uncertain it is within the rage of the test-pumpings by Ramadhani, M. M. (2013) and a larger extraction is questionable. The groundwater simulation model shows only small changes in waterhead further than 100 meters from a simulated pumping well, comparing natural condition and extraction at any rate (compare Figure 13 to Figure 15). Comparing Figure 14 with Figure 16,17,19,20 the cone of depression is obvious and has an approximate significant extent of 40-60 m, however changes in waterhead can easily be seen in the cross-section Figures (14 and 16-17 and 19-20) with extensive pumpage. The impacts in velocity direction due to pumping were according to simulations small (see Figure 22 and Figure 23) but velocity magnitude increased with pumpage. The fact the one third of the year is very dry is not considered during simulation (since dried cells did not converge) but might have an impact of possible extraction rate during the actual period. The effects of annual climate differences depends on aquifer robustness such as depth and characteristics. Pumping with well 1 or 2 did not have a significant impact for simulation.

7.3.2 Hydrogeological properties

The aquifer is assumed to be a confined aquifer as the previous drilling and magnetic survey investigators states that water is found in either fraction or weathered shales. The drilling report by Ramadhani, M.M (2013) also shows a layer of clay above the water transmitting layer. MODFLOW is using Darcy's law which assumes a homogeneous environment for each cell, and since no accurate knowledge about geological formations were known one layer was set with the same hydraulic conductivity. No natural geological unit of that size is totally homogeneous. The input values were isotropic, same at all locations, but that is also realistic in natural condition. However due to high elevation fall groundwater assumingly flows towards the location of the constant head applied at layer 1, towards the valley. Data regarding the aquifers characteristics on the hilltop was found in the magnetic survey and was used for simulation. Since there were no hydrogeological data of the suggested borehole locations in the valley aquifer thickness was set to 50 m at a depth of 20 m, values within the range found in Ramadhani, M. M. (2013) report. The choose of shales as a geologic entity in the valley is mainly because it is stated in the report from Shinhu, R. (2016) that it is likely. Modulation with different depth of aquifers shows, as Equation 8 states, that the depth of the aquifer is one of the parameters that determine the possible subtracted groundwater volume. The aquifer characteristics is only speculative in an environment of unlimited variations, but these values were found by iteration for a converging simulation model. According to simulation the piezometric head in the well without pumping is higher than the aquifer depth meaning it is initially under pressure, but since the level does not reach the surface the simulated well is not artesian (see Figure 8). The applied constant head areas in layer 2 did not have an effect of pumping capacity, the main factor of pumpage was aquifer thickness (hydraulic conductivity was not a varying parameter).

7.3.3 Constant head boundary and flow chart

The adjustment added to the model were constant waterhead boundaries (in layer 1 and 2) and a draining river. All cells were flooded without excessive drainage through the river boundary. Since the annual infiltration of 89 mm is regarding runoff the draining river is only a way to drain the model from excessive water and may be seen as exfiltration. The constant-head boundaries of 1450 masl and 1530 masl (in layer 1) were added to adjust unrealistic values of water head isolines over 1000 masl in the original simulation. The impacts of these adjustments is partly shown in Figure 20, where the flowchart shows difference between given and taken volume for all constant head boundaries as 55 m^3/day drainage. No water is added to the flowbudget through these boundaries and Figure 20 shows that the bulk part leaves the model through river leakage. To investigate the difference a simulation without the constant head boundaries of 1450 masl and 1530 masl was runned and result showed no significant difference in possible extraction rate or waterhead isolines closer to the pumping wells. The constant head set at layer 1 foremost function is draining the simulation and stimulate the flow direction, which can be seen in Figure 22, which further confirms that the constant-head boundaries at layer 2 does not affect the groundwater overall direction.

7.4 Sustainable withdrawal

The socio-ecologic sustainability of 50% withdrawal is highly questionable. Ponce., V (2007) states that the global average of deep percolation is 2% of total infiltration in a river basin. However Alley M.W et al (2013) argues that the sustainability and consequences have to be determined by the population involved. An inventory of users and stakeholders could be made for involving all users in decision making, however such inventory and agreement might be hard to meet.

With a fresh-water system consumption might increase. To not overexploit the groundwater resource a ration might be needed. This thesis does not take into account the part of Chonyonyo's population that already access fresh-water from pumping wells on the ridge and rain-harvest systems, which makes the demand smaller than calculated for.

Furthermore the analysed basin is a subcatchment to a larger basin and contribute with approximately 1/5th of the water discharge at merging point (1 km downstream the location of suggested boreholes). The contributing area to runoff at the merging point is 10 -18 km^2 (see Figure 10). Therefore impacts of larger extraction might not have dramatic impacts downstream the merging point. Groundwater simulation shows that the impact of pumpage is limited further away from the pumping well, why the larger impact would be the cone of depression and the area 1 km downstream pumping site to the merging discharge point. Another idea is to move the well to merging point, which would imply a 1 km longer pressured pipeline. The difference would be that the effects on surface waters and ecosystems in the subcatchment decrease, especially important to consider the existing waterhole and its location, since it might dry out. To recharge the aquifer greywater from Chonyonyos inhabitants could be emitted back to the catchment for infiltration as one of Alley W.M's strategies imply. Another applicable strategy of Alley W.M et al (2013) is spatial distribution, meaning that several pumping wells may have a positive contribution for sustainable groundwater management. However several pumping wells would increase implementation costs.

8 Conclusions and recommendations

The analysis show, within assumed parameter limits, that with a catchment area of 3,09 km^2 the total infiltration volume will be 275700 m^3, which meet Chonyonyo's demand of freshwater according to UN's absolute minimum limit of 20 liters/day and person. The extraction of total annual infiltration would be 50% which is not considered a sustainable outtake. However the catchment is a subcatchment to a larger basin why the impact of 50% withdrawal has to be investigated. Accurate logging and collection of data is needed once pumping starts for better mapping consequences of high extraction. According to groundwater simulations the aquifer's transmissivity is the limiting factor considering extraction rate. To meet the demand several wells have to be constructed around the catchment. The investigation of the potential borehole location showed that one location has a catchment 190 times the size of the other, however if the borehole site matters for pumping depends upon aquifer characteristics, both locations may extract from the same aquifer.

Further investigation is needed, this thesis recommend a test-pumping at preferable site, conducted in the same manner as the previous test-drilling 32 km north-east of the study-site (Ramadhani, M. 2013) which includes accurate logging of geologic layers and groundwater yield.

9 References

References

[1] Alley W.M., Reilly T.E., and Franke O.L. (11 01 2013) *Sustainability of Ground-Water Resources*, Retrieved 13 09 2017, from United States Geological Survey: https://pubs.usgs.gov/circ/circ1186/

[2] ASTER GDEM 2 READ ME (10, 2011) *Advanced Spaceborne Thermal Emission And Reflected Radiometer (ASTER). Global Digital Elevation Model (GDEM)*,

[3] The Earth Observatory, NASA (2017). *Measuring Vegetation (NDVI and EVI)*, Retrieved 10 20, 2016, from EOS Project Science Office, NASA Goddard Space Flight Center: www.earthobservatory.nasa.gov/Features/Measuring Vegetation/measuringvegetation2.php

[4] Engineers of the Earth, (2013) *Waterwell project in Bukoba District, Tanzania*,

[5] Engineers Without Borders, Malm (11 07 2016) *Chonyonyo Water Project*,

[6] ESRI, (2017) *Data classification methods*, Retrieved 10 10 2016 from ArcGIS Pro: http://pro.arcgis.com/en/pro-app/help/mapping/symbols-and-styles/data-classification-methods.htm

[7] FAO (2014) *Kagera Agro-Ecosystems*, Retrieved 10 20, 2016, from Food and Agriculture Organization of the United Nations: http://www.fao.org/in-action/kagera/home/en/

[8] FAO (2017) *Background information on Natural Resources in Kagera River Basin*, Retrieved 10 20, 2016, from Food and Agriculture Organization of the United Nations: http://www.fao.org/fileadmin/templates/nr/kagera/Documents/Suggest edreadings/nrinfokagera.pdf

[9] Fetter. C, (1994) *Applied Hydrogeology*, New Jersey: A Simon and Schuster company

[10] Google Earth Images (2017) *CNS /Airbus*, Retrieved 03 20 2017 from Google Earth Pro, 2017

[11] Heath, R.C., (1983) *Basic ground-water hydrology*, U.S. Geological Survey Water-Supply Paper 2220, 86p.

[12] Ministry of water and irrigation (10 2016) *Water sector development program*, Retrieved 13 09, 2017, from United Republic of Tanzania: http://www.maji.go.tz/?q=en/filebrowser/download/27537

[13] MSU (2017) *Horton's infiltration model*, Retrieved 12 20, 2016, from Michigan State University: http://www.egr.msu.edu/classes/ce421/lishug/text20book.pdf

[14] NASA (03 2013) *The Electromagnetic Spectrum*, Retrieved 12 20, 2016, from National Aeronautics and Space Administration, US: https://imagine.gsfc.nasa.gov/science/toolbox/emspectrum1.html

[15] NAU (2015) *Homogeneity and Isotropy*, Retrieved 12 20, 2016, from Northern Arizona University: http://jan.ucc.nau.edu/ doetqp-p/courses/env302/lec12/LEC12.html

[16] NRC (2017) *Satellite Imagery and Air Photos*, Retrieved 12 20, 2016, from Government of Canada: http://www.nrcan.gc.ca/earth-sciences/geomatics/satellite-imagery-air-photos/10782

[17] Richards, J. A., and Jia, X. (2006) *Remote sensing digital image analysis*, Berlin:Springer

[18] Ramadhani, M. M. (2013) *Completion report for eight (8) boreholes at Karagwe district in Karagera*, Karagwe district council

[19] Shinhu, R. (2016) *Application of Geophysical methods in locating groundwater potential sites at Chonyonyo village in Karagwe district - Kagera region*, Chonyonyo Geophysical survey report

[20] SMHI (09 17 2013) *Nederbord*, Retrieved 07 15 2016 from Sveriges Meteorologiska och Hyrdologiska Institut: https://www.smhi.se/kunskapsbanken/meteorologi/nederbord-1.361

[21] SMHI (06 08 2017) *Avdunstning*, Retrieved 07 15 2016 from Sveriges Meteorologiska och Hyrdologiska Institut: https://www.smhi.se/kunskapsbanken/hydrologi/avdunstning-1.30720

[22] Svenskt Vatten (01 2016) *P110 - Avledning av dag-, drn- och spillvatten*, Stockholm: Svenskt Vatten

[23] Tanzania Meteorological Agency (2017) *Data Analysis Tool, Maproom*, Retreived 10 10 2016 from Tanzania Metrological Agency, United Republic of Tanzania: http://maproom.meteo.go.tz/maproom/Climatology/ClimateAnalysis/monthl

[24] USGS (2005) *MODFLOW-2005, The U.S. Geological Survey Modular Ground-Water Modelthe Ground-Water Flow Process* , Retrieved 12 20, 2016, from USGS:
$http://inside.mines.edu/\ epoeter/583CSM/DOC4_MODFLOW2005-TM6$
$A16.pdf$

[25] USGS (2016, 12 09) *Aquifers and Groundwater*, Retrieved 10 20, 2016, from US Geological Survey: https://water.usgs.gov/edu/earthgwaquifer.html

[26] USGS, Earth Explorer (2017) *Landsat 8*, Retrieved 10 20, 2016, from United States Geological Survey: https://earthexplorer.usgs.gov/

[27] UN (2017) *The sustainability goals*, Retrieved 10 20, 2016, from Unite Nations: http://www.un.org/sustainabledevelopment/water-and-sanitation

[28] Unicef (2013) *Eastern and Southern Africa - Gender and water, sanitation and hygiene (WASH)*, Retrieved 10 20, 2016, from Unicef, Unite Nations: https://www.unicef.org/esaro/7310GenderandWASH.html

[29] UNPF, (03 19, 2013) *More prople move to urban areas as Tanzanian population gallops*, Retrieved 10 20, 2016, from United Nations Population Fund: http://tanzania.unfpa.org/en/news/more-people-move-urban-areas-tanzanian-population-gallops-0

[30] Volker, W (1998). Automatic classification of remote sensing data for GIS database revison. *International society for photogrammetry and remote sensing*, 641-648

[31] WaterAid (2017) *Tanzania - The crisis*, Retrieved 10 20, 2016, from WaterAid: http://www.wateraid.org/where-we-work/page/tanzania

[32] WHO (07 2017) *Drinking-water*, Retrieved 06 20, 2017, from WHO: http://www.who.int/mediacentre/factsheets/fs391/en/

[33] Zemadim et al (2011) *Evaporation Modelling in Data Scarce Tropical Region of the Eastern Arc Mountain Catchments of Tanzania*, Department of Water Resources Engineering, University of Dar es salaam, Tanzania

10 Appendix

10.1 Appendix I

10.1.1 Equation for second layer

Equation used to calculate geological layers, second layer being a water transmitting material.
First layer

$$H_1 = \frac{(H_X - H_{MIN})}{(H_{MAX} - H_{MIN})} * 60 + 20 \tag{10}$$

Second layer

$$H_2 = \frac{(H_X - H_{MAX})}{(H_{MAX} - H_{MIN})} * 40 + 10 \tag{11}$$

H_1= Thickness of first layer at the given point x
H_2= Thickness of second layer at the given point x
H_X= Altitude at a given point x
H_{MIN}= Minimum altitude of the catchment (1365 masl)
H_{MAX}= Maximum altitude of the catchment (1625 masl)

Thickness of layers varying with altitude, according to equations above. Below is an illustration of the relationship between thickness of the geological layer and altitude.

10.2 Appendix II

10.2.1 Excel calculations

Excel calculations for hydrological budget and annual infiltration volume vs. demand/supply

	jan	feb	mars	april	maj	juni	juli	augusti
P/mån	65	71	124	151	91	5,5	3,7	19
Temp max	28	28,3	27,5	26,5	26,5	27,5	28	28,5
Temp min	12,5	12,5	13	13	12,5	12,1	12	12,2
Ti	20,25	20,4	20,25	19,75	19,5	19,8	20	20,35
Ti'	8,3116435	8,405034	8,3116435	8,0029	7,850039	8,034	0,6339	7,54731

PE, Ei	180,57944	182,27115	180,57944	174,96433	172,17074	175,52417	177,76726	181,70688
	180,57944							
P/PE	0,3599524	0,3895296	0,6866784	0,863033	0,5285451	0,0313347	0,0208137	0,104564
KVOT	1,0628103	1,0731884	1,2130652	1,3209186	1,1310879	1,0004908	1,0002166	1,005452
AE/PE	0,3386798	0,3629648	0,5660688	0,6533582	0,4672891	0,0313193	0,0208092	0,103997
AE	61,15861	66,158004	102,22039	114,31438	80,453514	5,4973019	3,6991988	18,896975
run-off and	3,8413903	4,8419965	21,77961	36,685616	10,546486	0,0026981	0,0008012	0,1030254

Figure 24: Excel calculations for actual evapotranspiration.

	september	oktober	november	december
P/mån	59,5	109	123	116
Temp max	29	27,5	27	27,5
Temp min	12,5	12,6	12,5	12,5
Ti	20,75	20,05	19,75	20
Ti'	42,499	106,27	127,6	117

PE, Ei	186,2312	178,32896	174,96433	177,76726
P/PE	0,3194953	0,6112299	0,7030004	0,6525386
KVOT	1,0497987	1,1720077	1,2223787	1,1940714
AE/PE	0,3043396	0,5215238	0,5751086	0,546482
AE	56,677533	93,002802	100,62348	97,146616
run-off and	2,8224665	15,997198	22,376516	18,853384

I	111	
b	2,4547218	
a	1	
	36	Ti<19,6
C	30	19,6<Ti<21
	16	Ti>21

Figure 25: Excel calculations for actual evapotranspiration

In kbm				
Monthly hy	P	AE	R	I
jan	200850	188980,1	4187,1154	7682,7806
feb	219390	204428,23	5277,7762	9683,993
mars	383160	315861,01	23739,775	43559,22
april	466590	353231,45	39987,321	73371,232
maj	281190	248601,36	11495,669	21092,971
juni	16995	16986,663	2,9409729	5,3962806
juli	11433	11430,524	0,8732871	1,6023616
august	58710	58391,651	112,29773	206,05088
september	183855	175133,58	3076,4885	5644,933
oktober	336810	287378,66	17436,946	31994,396
november	380070	310926,57	24390,402	44753,032
december	358440	300183,04	20550,189	37706,769
				275702,38

In mm				
Monthly hy	P	AE	R	I
jan	65	61,15861	1,3550535	2,4863368
feb	71	66,158004	1,7080182	3,1339783
mars	124	102,22039	7,682775	14,096835
april	151	114,31438	12,940881	23,744735
maj	91	80,453514	3,7202813	6,8262043
juni	5,5	5,4973019	0,0009518	0,0017464
juli	3,7	3,6991988	0,0002826	0,0005186
august	19	18,896975	0,0363423	0,0666831
september	59,5	56,677533	0,9956273	1,8268392
oktober	109	93,002802	5,6430245	10,354173
november	123	100,62348	7,8933341	14,483182
december	116	97,146616	6,6505466	12,202838
Total infiltration in mm				89,22407

Total catchment-area	3,09	km2	
	3090000	m2	
Weighted run-off coeff	0,3527508		
Infitration coefficient	0,6472492		
Infilteration	275702,38	m3	
Daily water demand	0,02	m3	
Members per family	5	persons	
Households	4000	st	
Total annual water den	146000	m3	< 275702

Figure 26: Excel calculations of annual infiltrated volume and demand from Chonyonyo.